agriculture

MDPI

Article

Low Doses of Anatase and Rutile Nanoparticles Differently Modulate Photosynthesis and Regulatory Genes: A Contribution to the Nanoagroindustry

Nuno Mariz-Ponte [1,2,*], Sara Sario [1,2], Rafael J. Mendes [1,2], Márcio Couto [1], Emil Gimranov [1,2], Marino Santos [1,2], Cristiana V. Correia [1,2], Anicia Gomes [1], Paulo R. Oliveira-Pinto [1,2], Isabel Amorim [1,3], Maria Celeste Dias [2,4], José Miguel P. Ferreira de Oliveira [5] and Conceição Santos [1,2]

1 Faculty of Sciences, University of Porto, Rua do Campo Alegre, 4169-007 Porto, Portugal; sara.sario@fc.up.pt (S.S.); rafael.mendes@fc.up.pt (R.J.M.); marciocouto8dn17@gmail.com (M.C.); up201804355@fc.up.pt (E.G.); up201804357@fc.up.pt (M.S.); cristiana.correia@fc.up.pt (C.V.C.); anicia.gomes@fc.up.pt (A.G.); up201606827@edu.fc.up.pt (P.R.O.-P.); mpamorim@fc.up.pt (I.A.); csantos@fc.up.pt (C.S.)

2 LAQV-REQUIMTE, Faculty of Sciences, University of Porto, Rua do Campo Alegre, 4169-007 Porto, Portugal; celeste.dias@uc.pt

3 GreenUPorto—Sustainable Agrifood Production Research Centre/Inov4Agro, Department of Biology, Faculty of Sciences, University of Porto, 4169-007 Porto, Portugal

4 Centre for Functional Ecology (CEF), Department of Life Science, University of Coimbra, Calçada Martim de Freitas, 3000-456 Coimbra, Portugal

5 LAQV-REQUIMTE, Laboratory of Applied Chemistry, Department of Chemical Sciences, Faculty of Pharmacy, University of Porto, R. Jorge de Viterbo Ferreira 228, 4050-313 Porto, Portugal; jmoliveira@ff.up.pt

* Correspondence: nuno.ponte@fc.up.pt

Abstract: Industrial applications of titanium dioxide nanoparticles (TiO_2 NPs) are wide, and their use in nano-fertilizing technology has been proposed in the last few years. Bioactivity evaluation of different TiO_2 NPs formulations is therefore crucial, not only to select the most appropriate formulation but also to validate potential agro-applications. In the current work, we compared the bioactivity of the two most used TiO_2 NPs formulations (anatase and rutile–anatase) on the photosynthesis of *Lactuca sativa*. Seeds were exposed to concentrations of 0, 10, and 50 mg L^{-1} of anatase (A) or rutile–anatase (RA). Germination rate was not affected by NPs, but root growth was stimulated mainly by RA50. Compared with control, RA showed positive effects on photophosphorylation-related parameters. A50 was more efficient in promoting the gas exchange phase (PN, Ci, gs, and E) and in stimulating the absorption of some nutrients. Expanding on the biochemical and physiological data, we show that RA50 stimulated several genes coding for proteins involved in the electron transport in thylakoids (*psbA*, *petB*, *petA*, *psaA*, *psaC*, *ndhA*, *ndhD*) and ATP synthesis (*atpA*, *atpB*). The transcript coding for the large subunit of RuBisCO (*rbcL*), was stimulated by lower concentration (RA10). This suggests that RuBisCO is highly sensitive to these NPs even at low doses. RA at low doses has been demonstrated to be the most promising NP. These discriminative effects of TiO_2 NPs, based on their formulation and dose, may present advantages for their use in the precision nanoagroindustry.

Keywords: bioactivity; crop growth; gene regulation; photosynthesis; titanium-dioxide nanoparticles

Citation: Mariz-Ponte, N.; Sario, S.; Mendes, R.J.; Couto, M.; Gimranov, E.; Santos, M.; Correia, C.V.; Gomes, A.; Oliveira-Pinto, P.R.; Amorim, I.; et al. Low Doses of Anatase and Rutile Nanoparticles Differently Modulate Photosynthesis and Regulatory Genes: A Contribution to the Nanoagroindustry. *Agriculture* **2022**, *12*, 190. https://doi.org/10.3390/agriculture12020190

Academic Editor: Urs Feller

Received: 30 November 2021
Accepted: 26 January 2022
Published: 28 January 2022

1. Introduction

Nanoagriculture is opening a new era in the agro-food industry by playing an emergent role in improving crop production, providing highly efficient and sustainable nanopesticides, nanofertilizers, and nanosensors [1–6]. Several metal-based nanoparticles (NPs), particularly silver (Ag), copper (Cu), iron (Fe), titanium (Ti), and zinc (Zn) NPs, are increasingly being used to promote crop germination and plant growth, to improve stress

tolerance, or in the amendment of agricultural soils [1,7,8]. Titanium dioxide nanoparticles (TiO_2 NPs), which are among the most promising NPs in nanoagriculture, have also demonstrated lower toxicity than other metal-NPs in maize and rice [9]. It has also been shown that these TiO_2 NPs can reduce the phytotoxicity of other metal contaminants such as Al and Pb in lettuce plants [10]. TiO_2 NPs occur as anatase, rutile, or brookite. Anatase (A) and rutile–anatase (RA) are the two most widely used formulations [11]. Anatase and rutile (R) differ in structure: A is constituted by a tetragonal form with four TiO_2 units, while the tetragonal form of the R is constituted by two TiO_2 units. In addition to these different structures, the optical, mechanical, and chemical proprieties are also significantly different, namely color and photocatalytic activity, which promote distinct application in the industry [12,13]. Thus, it is expected that they may also differently influence plant growth [14,15]. TiO_2 NPs added to soil and hydroponic systems have been reported to be absorbed by plants from the roots and translocate throughout of plant [16,17]. The uptake mechanism of these TiO_2 forms remains unclear, although it has been suggested that it uses the same transporters of other metals [18,19]. Previous studies have shown that A is less genotoxic than RA, and positively influences lettuce and basil seedlings' growth [14]. Usage of anatase NPs may promote cold tolerance in chickpeas and increase crop productivity [20]. The changes in plant physiology may be due to TiO_2 NPs' ability to shift molecular pathways in plant organs, such as leaves and roots [21]. These NPs may also increase the adhesion of beneficial soil bacteria to the roots and help the plant's defense mechanisms [22].

Despite their evident potential for crop growth, a detailed explanation of how TiO_2 NPs influence plant photosynthesis is still lacking [23]. However, it has been reported to improve nitrogen metabolism, chlorophyll content, and photosynthetic performance [24,25]. In vitro studies showed that anatase NPs decreased oxidative stress levels and elevated the oxygen evolution rate in chloroplasts exposed to UV-B radiation, which supports the protective role of these NPs [26]. RA NPs showed antioxidant properties and improved photosynthetic performance in oilseed rape plants [27]. Moreover, Gao et al. [28] showed that A induced conformational changes in RuBisCO activase and enhanced its activity in spinach.

However, the effects of TiO_2 NPs on energy and carbohydrate-related metabolism were also contradictory. At doses as high as 750 mg kg^{-1}, RA (coated with Al_2O_3) decreased the levels of chlorophylls but increased total sugar and reducing-sugars compared to unexposed plants [29]. Doses between 100–500 mg L^{-1} of A NPs applied to rice decreased starch and sucrose metabolism, compromising the glyoxylate and dicarboxylate metabolisms, while stimulating the Krebs cycle and the pentose-phosphate pathway [30]. In general, these NPs have shown the potential to improve the light-harvesting complex II (LHCII), enhance light absorption and transport, and consequently improve photosynthetic metabolism [31–33]. These data suggest that high doses of TiO_2 NPs have a profound impact on energetic pathways, which must be taken into consideration in nanoagriculture strategies.

Current data show also that TiO_2 NPs phytotoxicity on lettuce may start at doses above 50 mg L^{-1} [34,35]. We hypothesize that low (non-toxic) doses of TiO_2 NPs will positively influence crops' growth and stimulate photosynthesis (by regulating one or both of photophosphorylation and Calvin cycle phases), and that TiO_2 NPs might also regulate photosynthesis-related key genes. We also hypothesize that these effects are dependent on the formulation and dose. To test this hypothesis and assess the potential phytotoxicity of these NPs, lettuce plants (a major dicotyledonous crop and widely used as an ISO model) were chronically exposed to different levels of TiO_2 NPs. After 21 days, plant water status and several photosynthesis-related parameters (gas-exchange, chlorophyll fluorescence, RuBisCO activity, pigments, and carbohydrates contents) were quantified.

2. Materials and Methods

2.1. NPs Supply, Characterization, and Solution Preparation

TiO_2 NPs (≥99.5% purity) were purchased from Sigma Aldrich, St. Louis, MO-USA. According to the supplier, A NPs have a size < 25 nm and a surface area ranging from 45–55 m^2 g^{-1}, and RA NPs, Aeroxide® P25 (Evonik, Essen, Germany) are composed of rutile and anatase (20:80) with an average size of 21 nm and a surface area ranging from 35–65 m^2 g^{-1}. A stock suspension (1 g L^{-1}) was prepared in deionized water and then sonicated (30 min). Based on previous works and predicted environmental concentrations [15,36,37], the final concentrations used to study photosynthetic effects for both NPs were: 0, 10, and 50 mg L^{-1}. Since most phytotoxic effects on crop plants have been reported for doses above 50 mg L^{-1} [35], the solutions were prepared by mixing the appropriate volumes of the growth medium (1/2 Hoagland, Sigma Aldrich, St. Louis, MO, USA) and the NPs-stock solution. Prior to use, all solutions were sonicated (~15 min). The characterization of these NPs, including the dispersion profile in suspension, was previously published [14].

2.2. Plant Material and Type of Substrate for Seed Exposure

Seeds of *Lactuca sativa* cv. 'Maravilla de Verano Canasta' (Vilmorin Jardin, Paris, France) were germinated on Petri dishes with 10 mL of water (control) or with A or RA solutions with concentrations of 10 or 50 mg L^{-1} (a total of 5 conditions) on cellulose Whatman paper (Cytiva, Maidstone, United Kingdom). After seven days of germination in the dark, 20 plantlets of each condition were transferred to larger containers with hydroponic medium, maintaining the same condition of exposure to NPs. Seedlings were then hydroponically grown on the respective medium with continuous aeration, with photosynthetic photon flux density (PPFD) emitted by fluorescent light lamps L 30W/77 FLUORA (OSRAM, Munich, Germany) at 250 µmol m^{-2} s^{-1}, temperature conditions around 22 + 2 °C, ~50% RH (relative humidity), and 16 h:8 h (day:night). To standardize the exposure conditions, all media were renewed three times a week, and the pH was maintained at ~5.6. All measurements were performed at the end of the exposure period, twenty-one days after the start of the exposure.

2.3. Plant Growth and Elemental Contents

Plant growth was determined by shoot and root length, and fresh and dry weight was determined using standard protocols [15]. Other morphological aspects (e.g., senescence, chlorosis, necrotic spots, abscission) were registered. After leaf incineration and H_2SO_2 dissolution of ashes, the levels of TiO_2 and of nutritional elements relevant to osmotic regulation and the photophosphorylation pathway, including K, Ca, Mg, Mn, Fe, Cu, and P, were measured by inductively coupled plasma mass spectroscopy (ICP-MS, Jobin Ivon JY70 Plus, Horiba, Kyoto, Japan).

2.4. Gas Exchange and PSII Efficiency

Fully expanded leaves of six plants per condition were used for gas exchange and chlorophyll a fluorescence determination. For gas exchange analysis, the gas-exchange portable photosynthesis system (LI-6400 Photosynthesis System, Li-COR, Lincoln, NE, USA) was used, operating in open mode. The analysis took place under atmospheric CO_2 conditions, and PPFD (~200 µmol m^{-2} s^{-1}) was supplied by an external halogen lamp (OSRAM, Munich, Germany). Transpiration rate (E, mol m^{-2} s^{-1}), stomatal conductance (gs, mol m^{-2} s^{-1}), net photosynthetic rate (PN, µmol m^{-2} s^{-1}), and intercellular CO_2 concentration (Ci, ppm) were determined as described in Dias et al. [37].

Photophosphorylation parameters were obtained by determining the minimal fluorescence yield (F0, PSII centers open) in 30 min dark-adapted expanded leaves (by applying a weak modulated light) with a fluorometer (LI-6400 Photosynthesis System, Li-COR, Lincoln, NE, USA). Then, a 0.7 s saturating-pulse of white light (>1000 µmol m^{-2} s^{-1}) was applied, and the maximal fluorescence yield of a dark-adapted sample (Fm, PSII centers

closed) was determined. The corresponding F0′ and Fm′ were also determined in leaves after adaptation to light for 30 min. The variable fluorescence values of the previous conditions (Fv = Fm − F0 and Fv′ = Fm′ − F0′) were estimated and the former was used to assess the maximum efficiency of PSII (Fv/Fm). Other parameters were also determined, including: photochemical quenching—qP [qP = (Fm′ − F′)/(Fm′ − F0′)], non-photochemical quenching—NPQ = [(Fm − Fm′)/Fm′], and the effective photochemical efficiency of ΦPSII [ΦPSII = [(Fm′ − F′)/Fm′] [38,39].

After gas exchange and PSII efficiency assessment, the same leaves were homogenized in acetone: 50 mM Tris buffer (80:20), and chlorophyll, carotenoid (car), and anthocyanin (ant) contents were determined according to Sims and Gamon [40].

2.5. Carbohydrate Content

Total soluble sugars (TSS) and starch were quantified by the anthrone method [41] and according to Osaki et al. [42], respectively.

2.6. Gene Expression

Total leaf RNA was isolated using the PureZOL™ RNA Isolation protocol (Bio-Rad, Hercules, CA, USA), according to manufacturer instructions. RNA samples were then treated with the Deoxyribonuclease I, Amplification Grade DNAse (Invitrogen™, Waltham, MA, USA), for reverse Transcriptase-PCR, where 1 µg total RNA was used to synthesize the first-strand cDNA with the NZY First-Strand cDNA Synthesis Kit (NZYTech™, Lisbon, Portugal) according to manufacturer's instructions. cDNA product was then treated with 1 µL NZY RNase H and stored at −20 °C.

The Lettuce Genome Resource database (https://lgr.genomecenter.ucdavis.edu/, accessed on 1 March 2016) was used to select the genes, and primers were designed using Primer 3 plus (https://primer3plus.com/, accessed on 1 March 2016). Primers for two reference genes previously analyzed by Borowski et al. [43] were designed as shown in Table 1: the β-tubulin gene (*β tub*) and the adenine phosphoribosyltransferase 1 (*apt1*) gene. Primers were also designed for genes implicated in photosynthesis-related processes (Table 1). For real-time quantitative polymerase chain reaction (RT-qPCR) reactions, 2.5 µL of cDNA, 5 µL of iTaq™ Universal SYBR® Green Supermix enzyme (Bio-Rad), and 2.5 µL of primers at 10 µM were mixed, in a total volume of 10 µL. Amplification was standardized, using the CFX96 Touch™ Real-Time PCR Detection System (Bio-Rad), and the following conditions were used: 95 °C for 1 min, followed by 40 cycles of 3 s at 95 °C and 30 s at 60 °C. The melting curve analysis ranged from 65 °C to 95 °C with increments of the temperature of 0.5 °C in 10 s per cycle. Gene expression was analyzed by the $2^{-\Delta\Delta CT}$ method [44].

Table 1. Primers used for gene expression analysis.

Gene Designation	Description	GenBank ID	Primers (5′–3′)
β tub *	β-tubulin, btub1	AB232704.1	F: AAATGTGGGACGCAAAGAAC R: TCATCCACCTCTTTCGTGCT
apt1 *	adenine phosphoribosyl transferase 1-like	XM_023900216.1	F: CGCCATTTACAAGCTTCATATTC R: ATCCCTGGCTTCGGAAAG
petB	cytochrome b6	NC_007578.1:74837–76254	F: ACAGGTGTGGTTCTGGGTGT R: GTGGATTGTCCCACACTAGCA
petA	cytochrome f	NC_007578.1:62045–63007	F: GATACGAAATAACCATAGCGGATG R: ATCCCTGGCTTCGGAAAG
psbA	photosystem II protein D1	NC_007578.1:c1540-479	F: GTGTAGCTTGTTACATGGGTCGT R: TCCTAGAGGCATACCATCAGAAAAG
psaA	photosystem I P700 chlorophyll a apoprotein A1	NC_007578.1:c41453-39201	F: ATGGCTAAGCGATCCGACT R: TCCAGATGCTCGCCAAAT
psaC	photosystem I subunit VII;	NC_007578.1:c116733-116488	F: TGTATCGGGTGTACGCAATG R: CAGGCGGATTCACATCTCTT

Table 1. *Cont.*

Gene Designation	Description	GenBank ID	Primers (5′–3′)
atpA	ATP synthase CF1 alpha subunit	NC_007578.1:28282–29808	F: TGTAGCTATTGGTCAAAAAGCATCT R: GCCAGAGCTGCTCCTGTATAA
atpB	ATP synthase CF1 beta subunit	NC_007578.1:c54296-52800	F: AACGAGAGGGATGGACGTAAT R: GTATAAAGGCAGGCGCAGAT
ndhA	NADH dehydrogenase subunit 1	NC_007578.1:c121081-118937	F: GCGCAGTCAAAATATGGTTTTT R: CGGTTTGATAACCTGCTACTAATT
ndhD	NADH dehydrogenase subunit 4	NC_007578.1:c116370-114868	F: ACGTCTTGTTTATCTCGACCAAA R: TGAGTGGTTTTGTTGCAGAAGT
rbcL	RuBisCO large subunit	AY874437.1	F: ATTTTGGCAGCATTTCGAGT R: CATCGGTCCACACAGTTGTC

* reference genes β-tubulin gene (*β tub*) and adenine phosphoribosyltransferase 1 (*apt1*).

2.7. Statistical Analysis

Except when specifically mentioned, 10 plants were used for the overall experiments, which were treated as individual samples or as pools (pigment and carbohydrate content determination and gene expression), all with at least 3 independent technical replicates. The values are presented as mean ± standard deviation. Comparisons between NP conditions and controls were based on the One Way ANOVA test. When data was statistically different, the Dunnett comparison test ($p < 0.05$) was also used. Multivariate analyses for data correlation were conducted based on principal component analysis (PCA) using the CANOCO for Windows v4.02 program (Canoco, Wageningen, The Netherlands).

3. Results

3.1. Germination, Growth, and Nutrition

Seed germination was not affected by the presence of TiO_2 NPs, as seeds reached a germination rate of 100% in all conditions. Likewise, no visible morphological changes were observed in seedlings exposed to A or to RA compared with the control.

Reduction of shoot length was observed in both groups of NPs-treated plants, with significant differences for A50 compared to the control, while between A- and RA-treated plants no changes were observed (Table 2). Regarding root length, plants exposed to both RA conditions showed a hormetic profile, with roots exposed to RA50 being two times longer than those exposed to RA10 ($p < 0.05$) (Table 2).

Table 2. Effects of A and RA treatments on length and biomass of shoots and roots. Different letters mean significantly different values ($p < 0.05$).

		Control	A10	A50	RA10	RA50
Length (cm)	Aerial part	6.85 ± 0.521^{b}	5.83 ± 0.650^{ab}	5.35 ± 1.150^{a}	6.42 ± 1.020^{ab}	6.27 ± 0.535^{ab}
	Root part	3.88 ± 1.036^{ab}	3.52 ± 0.776^{a}	3.82 ± 2.062^{ab}	2.33 ± 0.816^{a}	5.68 ± 0.788^{b}
Fresh matter (mg)	Aerial part	195.5 ± 64.61^{ab}	259.6 ± 91.45^{b}	151.0 ± 74.41^{ab}	261.2 ± 49.61^{b}	97.4 ± 17.17^{a}
	Root part	28.3 ± 1.71^{ab}	35.8 ± 12.38^{ab}	21.6 ± 10.11^{a}	45.0 ± 9.77^{b}	20.0 ± 4.69^{a}
Dry matter (mg)	Aerial part	4.5 ± 1.10^{a}	7.2 ± 3.27^{a}	5.0 ± 2.24^{a}	7.8 ± 2.39^{a}	3.8 ± 1.30^{a}
	Root part	1.0 ± 0.00^{a}	1.2 ± 0.45^{a}	1.0 ± 0.00^{a}	1.2 ± 0.45^{a}	1.25 ± 0.25^{a}

Interestingly, in both A10 and RA10 groups, an increase in the fresh matter of the shoots and roots was consistently observed, while in A50 and RA50 this effect was lost; displaying lower mean values of fresh matter compared to the control (Table 2). These observations reveal a quadratic response between the doses in both organs. Regarding dry matter, no differences were found between the treatments in shoots and roots. Comparing the FM/DM ratios of both aerial and root parts, there was an evident trend of these ratios increasing in A10 and A50 as well as in RA50.

The leaf elemental analysis shows that TiO_2 is absent or residual in leaves and that exposure to A10/50 significantly increased ($p < 0.05$) Ca, Fe, and Mn contents. The effect of RA on elemental content was less evident, but both doses slightly increased Fe and Mn, while RA50 decreased Ca and P levels (Table 3).

Table 3. Effects of A and RA treatments on leaf TiO_2 accumulation and composition of nutrients crucial for photosynthesis or osmotic balance. Nd.: not detected. Different letters mean significantly different values ($p < 0.05$).

mg·gDM^{-1}	Control	A10	A50	RA10	RA50
Ca	2.45 ± 0.291 ^{ab}	3.78 ± 0.334 ^{c}	3.62 ± 0.076 ^{c}	2.70 ± 0.882 ^{b}	1.84 ± 0.399 ^{a}
K	47.49 ± 9.588 ^{a}	42.52 ± 2.348 ^{a}	43.74 ± 3.123 ^{a}	42.73 ± 7.857 ^{a}	37.01 ± 6.476 ^{a}
Fe	0.10 ± 0.029 ^{a}	0.17 ± 0.022 ^{b}	0.16 ± 0.037 ^{b}	0.14 ± 0.031 ^{ab}	0.14 ± 0.025 ^{ab}
Mg	7.68 ± 0.517 ^{a}	8.05 ± 1.588 ^{a}	8.90 ± 0.879 ^{a}	8.00 ± 1.268 ^{a}	7.33 ± 0.635 ^{a}
P	16.74 ± 0.273 ^{b}	14.40 ± 0.622 ^{ab}	13.44 ± 1.209 ^{ab}	14.76 ± 3.902 ^{ab}	12.38 ± 2.162 ^{a}
Mn	0.68 ± 0.052 ^{a}	0.84 ± 0.139 ^{b}	0.91 ± 0.055 ^{b}	0.85 ± 0.090 ^{b}	0.90 ± 0.064 ^{b}
Ti	Nd.	Nd.	2.5×10^{-6}	Nd.	6.7×10^{-6}

3.2. Photosynthetic Performance

In the control group, the levels of chlorophyll *a* (chl*a*) were 0.124 ± 0.0129 µmol gFM^{-1} and those of chlorophyll *b* (chl*b*) were approximately half (0.053 ± 0.0053 µmol gFM^{-1}). These levels only increased ($p < 0.05$) with RA10 treatment, in a proportional way, thus maintaining the chl*a*/chl*b* ratio (Table 4). The levels of carotenoids and anthocyanins were also not significantly affected by any NP treatment.

Table 4. Effects of A and RA treatments on chlorophylls, carotenoids, and anthocyanin contents. Different letters mean significantly different values ($p < 0.05$).

µmol gFM^{-1}	Control	A10	A50	RA10	RA50
Chl*a*	0.124 ± 0.013 ^{a}	0.122 ± 0.015 ^{a}	0.126 ± 0.008 ^{a}	0.162 ± 0.016 ^{b}	0.126 ± 0.016 ^{a}
Chl*b*	0.053 ± 0.005 ^{a}	0.052 ± 0.005 ^{a}	0.055 ± 0.005 ^{a}	0.070 ± 0.007 ^{b}	0.054 ± 0.008 ^{a}
Chl*a*/*b* ratio	2.324 ± 0.010 ^{a}	2.317 ± 0.037 ^{a}	2.321 ± 0.064 ^{a}	2.320 ± 0.015 ^{a}	2.333 ± 0.061 ^{a}
Anthocyanins	0.008 ± 0.002 ^{a}	0.007 ± 0.002 ^{a}	0.009 ± 0.002 ^{a}	0.008 ± 0.001 ^{a}	0.009 ± 0.004 ^{a}
Carotenoids	0.051 ± 0.005 ^{a}	0.052 ± 0.007 ^{a}	0.055 ± 0.004 ^{a}	0.068 ± 0.008 ^{a}	0.054 ± 0.008 ^{a}

Regarding the F_v/F_m ratio, all plants showed a ratio of ~0.83. Moreover, among the most relevant photophosphorylation-related parameters in dark-adapted leaves (F_0, F_m, and F_v), no changes were observed between the NPs treatments and the control (Table 5). Contrarily, the corresponding parameters in light-adapted leaves ($F_{0'}$, F_m', and F_v') showed a significant decrease ($p < 0.05$) in plants exposed to A10 (Table 5), while in plants treated with A50 these values were close to those of the control.

The parameters F_v/F_m, F_v'/F_m', ΦPSII and qP, did not vary between NP-exposed plants and the controls. NPQ was statistically significantly stimulated ($p < 0.05$) by the presence of A10 (3× higher than the control), with slight increases in the other conditions (Table 5).

Table 5. Effects of A and RA treatments on chlorophyll a fluorescence. Different letters mean significantly different values ($p < 0.05$).

Parameter	Control	A10	A50	RA10	RA50
F_0	70.3 ± 10.31 ^{a}	62.6 ± 6.72 ^{a}	68.7 ± 15.37 ^{a}	75.2 ± 18.24 ^{a}	69.8 ± 8.12 ^{a}
F_m	433.8 ± 84.34 ^{a}	362.0 ± 44.93 ^{a}	420.5 ± 116.63 ^{a}	466.2 ± 145.08 ^{a}	437.0 ± 74.75 ^{a}
F_v	363.4 ± 75.08 ^{a}	299.38 ± 39.58 ^{a}	351.8 ± 101.33 ^{a}	391.0 ± 127.38 ^{a}	367.3 ± 66.82 ^{a}
F_v/F_m	0.84 ± 0.014 ^{a}	0.83 ± 0.011 ^{a}	0.83 ± 0.011 ^{a}	0.83 ± 0.024 ^{a}	0.84 ± 0.012 ^{a}
$F_{0'}$	27.0 ± 8.77 ^{b}	9.4 ± 5.19 ^{a}	26.0 ± 9.86 ^{b}	17.8 ± 7.52 ^{ab}	26.0 ± 13.60 ^{b}

Table 5. *Cont.*

Parameter	Control	A10	A50	RA10	RA50
F_m'	151.9 ± 35.43 ^{b}	70.1 ± 36.38 ^{a}	133.2 ± 46.89 ^{ab}	123.7 ± 34.59 ^{ab}	148.4 ± 59.51 ^{b}
F_v'	124.8 ± 28.27 ^{b}	60.7 ± 32.37 ^{a}	107.2 ± 37.98 ^{ab}	105.8 ± 32.46 ^{ab}	122.4 ± 46.66 ^{b}
F_v'/F_m'	0.82 ± 0.032 ^{a}	0.86 ± 0.039 ^{a}	0.80 ± 0.028 ^{a}	0.85 ± 0.061 ^{a}	0.83 ± 0.033 ^{a}
Φ_{PSII}	0.44 ± 0.085 ^{a}	0.54 ± 0.067 ^{a}	0.48 ± 0.133 ^{a}	0.46 ± 0.070 ^{a}	0.49 ± 0.074 ^{a}
qP	0.54 ± 0.113 ^{a}	0.63 ± 0.058 ^{a}	0.59 ± 0.144 ^{a}	0.54 ± 0.081 ^{a}	0.59 ± 0.078 ^{a}
NPQ	1.91 ± 0.417 ^{a}	6.02 ± 4.201 ^{b}	2.28 ± 0.617 ^{a}	2.83 ± 1.039 ^{ab}	2.19 ± 0.782 ^{a}

Regarding gas-exchange analysis, the data show that both A and RA formulations decreased PN (Figure 1a), with A50, RA10, and RA50 being the treatments showing the most acute effect ($p < 0.05$). Stomatal conductance (gs) was significantly stimulated only at A50 ($p < 0.05$), which is in line with the increase in Ci for that condition (Figure 1b,c). Transpiration rate (E) was higher ($p < 0.05$) for both A50 and RA50 (Figure 1d).

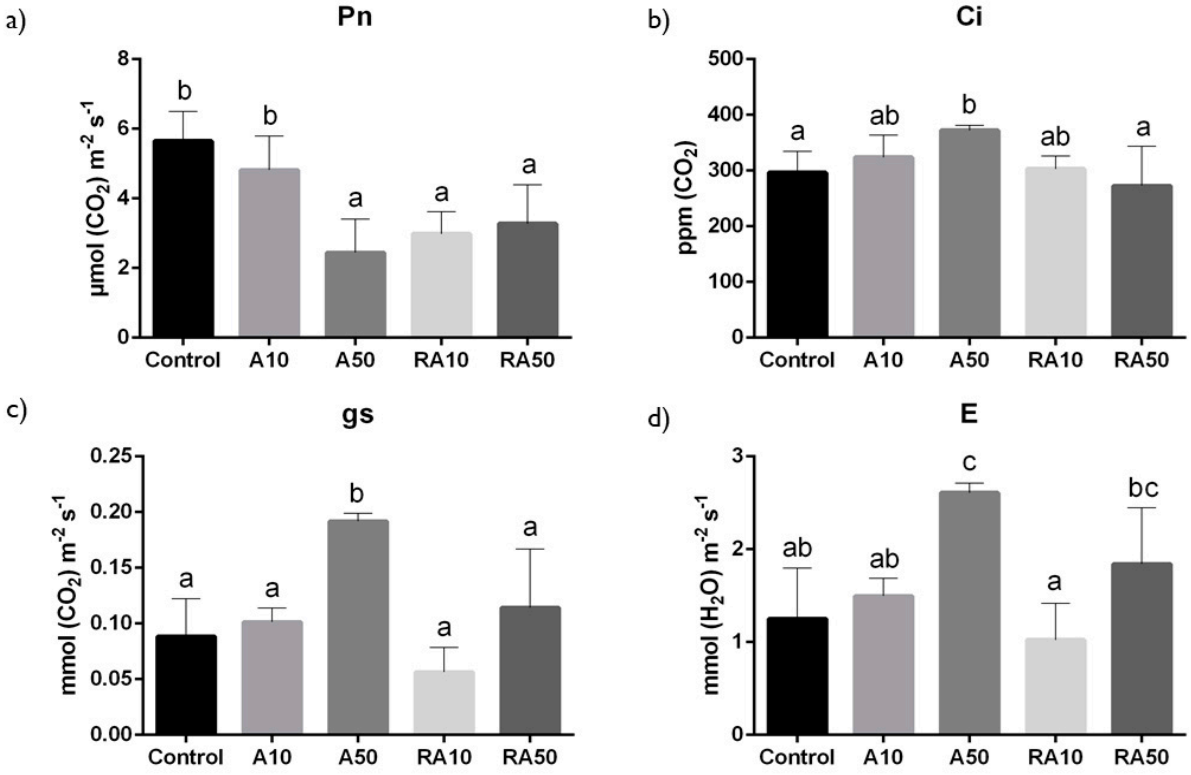

Figure 1. Effects of A and RA treatments on gas-exchange-related parameters: (**a**) net photosynthetic rate—PN; (**b**) internal CO_2 concentration—Ci; (**c**) stomatal conductance—gs; (**d**) transpiration rate—E. Different letters mean significant differences ($p < 0.05$).

Carbohydrate analysis (Figure 2) showed that starch was only significantly decreased ($p < 0.05$) to ~50% of the values of the control in RA50 (Figure 2b. Contrarily, the amount of TSS was significantly increased only in this condition (Figure 2a).

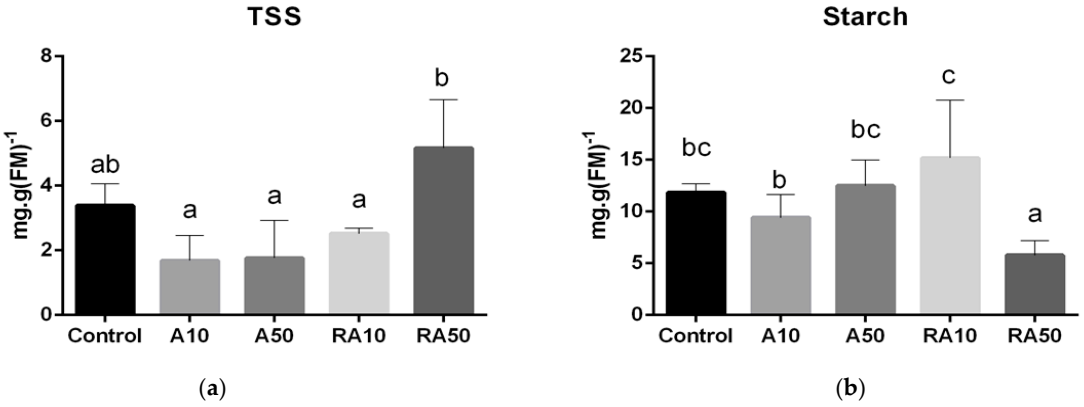

Figure 2. Effects of A and RA treatments on the levels of (**a**) TSS: total soluble sugars; (**b**) starch. Different letters mean significant differences ($p < 0.05$).

3.3. Gene Expression

Despite a trend of decreasing at low NP doses, the expression of the *psbA* gene, coding for a subunit of protein D1 of the PSII light-harvesting complex, was influenced neither by A nor by RA (Figure 3a).

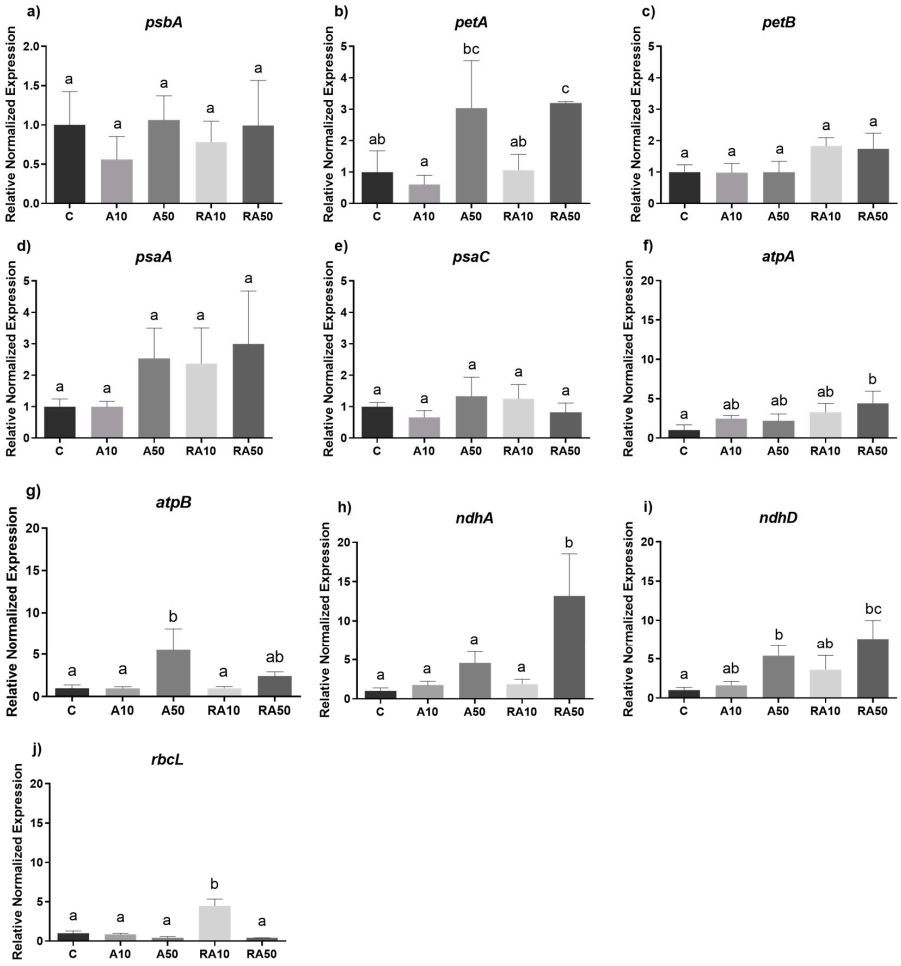

Figure 3. Effects of A and RA treatments on the expression of genes: (**a**) *psbA*, (**b**) *petA*, (**c**) *petB*, (**d**) *atpA*, (**e**) *atpB*, (**f**) *psaA*, (**g**) *psaC*, (**h**) *ndhA*, (**i**) *ndhD*, and (**j**) *rbcL*. Different letters mean significantly different values ($p < 0.05$).

The levels of *petA* transcripts, a gene coding for a subunit of the cytochrome f, significantly increased with A50 and R50 treatments ($p < 0.05$, Figure 3b). The transcript levels of the *petB* gene, coding for cytochrome b6, were not influenced by A nor RA, although a trend for increased expression in RA was observed (Figure 3c). The transcript levels of the *psaA* gene (coding for the PSI700 chl *a* apoprotein A1 subunit) and the *psaC* gene (coding for the PSI iron-sulfur center subunit) did not change in response to A or RA (Figure 3d,e), despite a trend of increasing for the former transcript.

The expression of *atpA* showed a tendency to increase in A (approximately two-fold), and particularly in RA where it reached significantly different expression at RA50 (four-fold change compared to the control, $p < 0.05$, Figure 3f). The transcript for another subunit of the ATP synthase complex, *atpB*, showed a tendency to increase particularly at the higher doses of NPs, being statistically significant in A50 (five-fold higher than the control, $p < 0.05$, Figure 3g). Regarding the *ndhA* and *ndhD* genes, coding for the NAD(P)H-quinone oxireductase subunits, the levels of the transcripts show a tendency to increase in A50 and RA50 (being statistically significant for the second, with a more than seven-fold increase compared to control, $p < 0.05$, Figure 3h,i). Finally, the transcript levels of the *rcbL* gene, coding a subunit of RuBisCO, were significantly enhanced in RA10 leaves (four-fold increase compared to control, $p < 0.05$, Figure 3j).

3.4. PCA Analysis

PCA showed a clear separation between control and NPs treatments (A10, A50, RA50), and between A10 and RA (Figure 4). PC 1 explained 34% of the variance and PC 2 41%. RA10 treatment is located on the lower left quadrant, together with the control, and the group mostly scores for photosynthetic pigments, starch and shoot length, and some chlorophyll *a* fluorescence indicators.

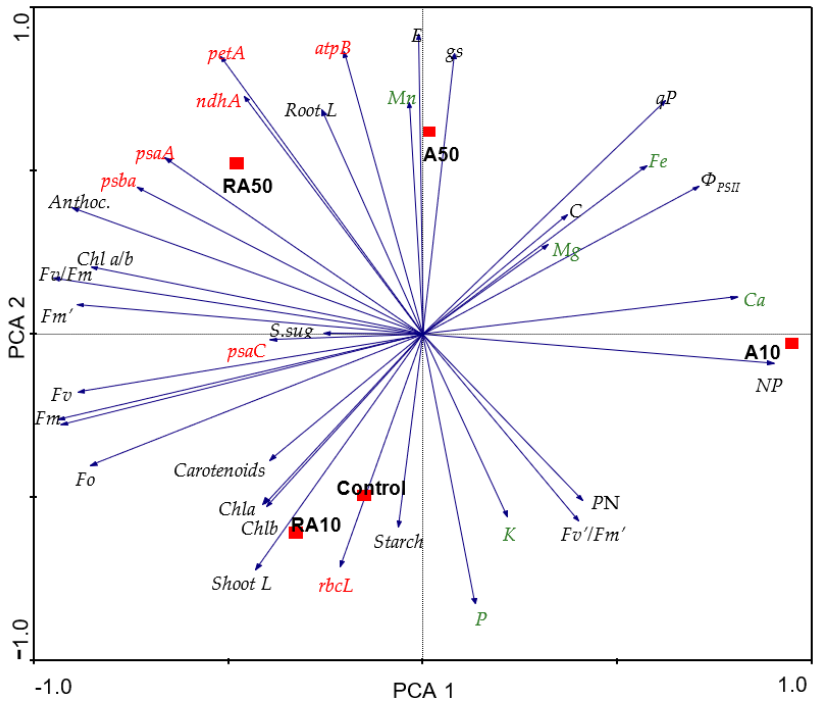

Figure 4. PCA biplot of A and RA treatment (10 mg·L^{-1} and 50 mg·L^{-1}) effects on lettuce plants. Loading plot for the first axis, PCA 1, explained 34% of the variance, and the second axis, PCA 2, explained 41%.

The RA50 is located in the upper left quadrant scoring mostly for photosynthesis-related genes (associated with proteins of the electron transport chain), anthocyanins, and chlorophyll a/b ratio as well as Fv/Fm and root length. On the upper right quadrant, A50

also scores for genes, E and gs. In the lower right quadrant, A10 scores for NPQ, for some nutrients, and eventually for PN and Fv'/Fm'.

4. Discussion

In this work, we demonstrate that the chronic exposure of lettuce seedlings/plants (21 days via root exposure) to low doses of A and RA may increase growth and biomass in crops (FM and DM), while higher doses increase root length. The increase in biomass may be attributed to the stimulation of photosynthesis, but the manner in which TiO_2 NPs interferes with photosynthesis in vivo is complex and dependent on NP formulation and dosage.

As photochemistry provides energy and reducing power for CO_2 assimilation, parameters related with this phase provide valuable information about productivity [39]. The PCA analysis shows that, despite the small trend of increasing pigments observed in most of the NP treatments, RA10 could positively influence its levels on lettuce leaves, reinforcing its beneficial effect for photosynthetic performance. In line with the data of Wang et al. [45], we suggest that the low doses used here of A either do not influence chlorophylls biosynthesis or slightly increase their biosynthetic pathways, while also stimulating important defense pathways (e.g., the xanthophyll cycle). RA increased chlorophyll levels in cucumber [46], while not affecting the chlorophyll and carotenoid contents in *Brassica campestris*, *Lactuca sativa*, and *Solanum lycopersicum* [47,48]. Another study showed that anatase increased chlorophyll contents in tomato plants [49]. Despite an evident stimulating trend, differences must be understood considering the cultivars, type of exposure, and dose, as pointed out by Zheng et al. [48].

Considering Fv/Fm, the values were ~0.83, which is close to the optimum value described in the literature for healthy unstressed plants [50], with lower values being associated with plants under stress. Our data show that the plants' potential quantum yield was not susceptible to either A or RA, which shows that the dosages used of the NPs exert little stress at this photochemical level. Likewise, the quantum yield baseline (F0/Fm), which is 0.16 in the control, was not significantly affected by the NP treatments, indicating that both A and RA maintain a balanced equilibrium between the reduction of plastoquinone QA and its reoxidation by QB. Interestingly, the PCA indicates a close relationship between RA50 and the genes coding for proteins of the electron transport chain, including cytochrome b6f (*petA*), *psbA*, a gene coding for the D1 protein of the PSII, *psaA*, *psaC* (coding for proteins of the PSI), the genes coding for the ATP synthase CF1 α and β subunits (*atpA* and *atpB*), and the NADH dehydrogenase subunits 1 and 4 (*ndhA* and *ndhD*). This positive relationship indicates a wide influence of RAs on the transcriptional regulation of genes coding for the photophosphorylation chain. Additionally, RA10 was the most efficient in stimulating gene coding for a subunit of RuBisCO (*rbcL*). TiO_2 NP-treated spinach evidenced a stimulus in RuBisCO and RuBisCO activase, which promoted RuBisCO carboxylation and increased the rate of photosynthetic carbon reaction [51]. This is the first comparative study of the influence of A and RA on the transcriptional regulation of genes coding for the photophosphorylation stage and RuBisCO.

Contrarily to what was observed in RA-treated plants, and as demonstrated in the PCA, A showed higher interference in the photochemical reactions, particularly A10 in light-adapted leaves, leading to higher changes in their photochemical status, comparing to the control. Minimal fluorescence values may increase when the PSII reaction centers are impaired or when the transfer of excitation energy from the antenna to the reaction centers is weakened [52]. The decrease of more than 50% in F0′ values in leaves exposed to A may suggest a lower number of active PSII reaction centers, as no significant decrease in chlorophyll contents was observed. The maintenance of F0′ close to F0′ control values in plants exposed to RA demonstrates that these NPs do not damage/inactivate the photosynthetic apparatus of the PSII reaction centers. Similarly, the stability of Photosystem II Efficiency [ΦPSII = (Fm′ − Fs)/Fm′] shows that these NPs do not target, or even slightly stimulate, the proportion of light absorbed by chlorophylls associated with PSII and used

in photochemistry. It has been documented that this parameter is affected by stressful conditions such as salinity and drought [53]. As initially calculated by Schreiber et al. [52], around 1 mol of photons leads to an excitation of ~1 µmol of chlorophyll electrons, with the efficiency of photosystem II (ΦPSII) being representative of the proportion of these electrons that will photochemically reduce $NADP^+$. From this, one may assume that the low doses of A and RA tested do not hinder Photosystem II efficiency, and that these low doses may even lead to a slight stimulation. It should be noted that only A10 increased the total non-photochemical heat dissipation, NPQ, and it may stimulate protective mechanisms against excessive energy in the chloroplasts. However, this effect might be reversed by higher concentrations.

The photochemical phase provides the necessary amounts of ATP and NADPH for the Calvin cycle. Data for gas-exchange parameters show that the decrease in PN observed at the higher doses of A and RA was not paralleled by changes in stomatal conductance (only increased in A50), meaning that it may rather be influenced by the existing higher internal CO_2 inside the leaf (Ci). The contribution of photorespiration (an essential process for C3 plants) to the changes of Ci in response to A and RA deserves further investigation. The water use efficiency (WUE) can be calculated from the ratio Pn/E, and the increase in E at A50 suggests that at higher doses, A may positively regulate the stomatal aperture at the cost of loss of water use efficiency, putatively increasing the tension of the xylem compared to the control and other treatments. On the other hand, an enhancement of stomatal aperture in high doses of A, not keeping up with the CO_2 assimilation rate, may be understood to be due to a TiO_2 role in the energy flux rate, and thus that opening the stomata may be helping the plant during the thermal dissipation [54]. Our data thus suggest that the accumulation of Ci in this condition and the decrease in CO_2 flux is not due to stomatal limitations, but to the influence exerted by higher doses of A on the Calvin cycle, this being the hypothesis under study.

Studies on wheat showed that RA induced alterations in ΦPSII, which might contribute to the detected impairments in PN [37]. Decreases in PN were also observed in the dicotyledon shrub *Clarkia unguiculata* when exposed to RA, with an increase of Ci [55]. However, this correlation was not found in lettuce exposed to the low doses of A and RA tested in this work. Significant improvement in PN, Ci, E, and gs was reported in *Brassica napus* plants sprayed with RAs [27]. These differences, regarding our results, may be related to the different exposure conditions used. We demonstrate here that under the same conditions of exposure, RA's effects on CO_2 assimilation differ from those reported in the literature for pure A. A consequence of PN decrease can be the impairment in Calvin cycle enzymes and carbohydrate production. RuBisCO catalyzes CO_2 assimilation by the carboxylation of ribulose 1,5-bisphosphate, and several reports have highlighted the positive effects of single pure anatase or rutile on PN, due to the improvement of RuBisCO activity and RuBisCO activase [28,51,56]. Negative results on RuBisCO activity were only reported by Zheng et al. [48] when using 6% RA, much higher dosages than those used here.

The observed change in the carbohydrate levels in plants exposed to RA was also reported in cucumber fruits [46]. The PCA analysis shows that starch content shares a close profile with some pigments (Chla/b, car) and a negative correlation with gs. Starch shows some negative correlation with soluble sugars, which may suggest that the interconversion of starch into sugars and vice-versa depends on the dose of NPs. Soluble carbohydrates are important for maintaining leaf cell turgor, but they also act as nutrients and as metabolite signaling molecules involved in a plant's reaction to stress [57]. The positive correlation of higher dosages of RA and A with transpiration and stomatal conductance shows that, at these doses, NPs are not absorbed by the root system in quantities high enough to block the cell wall pores and/or compromise water uptake. In maize plants hydroponically exposed to RAs, a reduction in water flow together with decreases in transpiration and biomass was observed [58]. Moreover, RA downregulated a gene that encodes for water transport in *Arabidopsis* [59], supporting the inference that the increase in soluble sugars may represent a strategy for maintaining leaf cell turgor [60] and coping more effectively with increased

transpiration and putative water loss. We report here that transcriptional changes are only evidenced at the doses of 50 mg L^{-1}, suggesting that, except for *rbcL*, the effects induced by 10 mg L^{-1} are predominantly biochemical and do not involve gene regulation. At higher concentrations, the effect of the NPs (namely RA) involves transcription regulation. In general, no/low phytotoxic effects were observed using photosynthetic endpoints. Besides the lower Pn for some concentrations tested (A50, RA10, RA50), other parameters such as chlorophyll, soluble sugars/starch, and biomass were not compromised under these conditions, and in some cases they were higher than the control. Thus, attending to these multiple approaches on the photosynthetic performance of lettuce, the concentrations used with both formulations were not able to generally impair plant production.

5. Conclusions

In conclusion, and as summarized in the PCA, these data show a clear distinction between the effects of the two TiO_2 NP formulations on the lettuce crop model (both A treatments score on the right side, while both RA treatments score on the left side). A exerts a beneficial influence on nutrients and on important parameters of gas exchange (e.g., qP, gs, and E, and RuBisCO genes), while RA correlates better with chlorophyll a fluorescence-related parameters and pigments. Moreover, the concentration effect is also evidenced, as the low dosages (10 mg L^{-1}) score in the lower region together with the control, while higher dosages (50 mg L^{-1}) score in the upper region. On the one hand, high doses of RA and A increased, in general, the expression of some genes related to the photosynthetic apparatus. On the other hand, it is shown that RA10 more evidently causes stimulation of photosynthetic pigments. This dual effect of TiO_2 NPs, also dependent on the formulation, allows the use of the best formulation/dose to selectively target a phase of the photosynthesis. Further studies should be carried out on environmental impacts and novel applications of these NPs for plant production. Their potential for agricultural use along with their putative risks for the food chain deserve further attention.

Author Contributions: Conceptualization, C.S.; methodology, N.M.-P., M.C., E.G., M.S., R.J.M., S.S., J.M.P.F.d.O., M.C.D., P.R.O.-P., C.V.C. and A.G; writing—original draft preparation, M.C.D., C.S., N.M.-P., S.S. and R.J.M.; writing—review and editing, M.C.D., C.S., N.M.-P., S.S., R.J.M., P.R.O.-P., C.V.C. and A.G.; supervision, C.S. and I.A. All authors have read and agreed to the published version of the manuscript.

Funding: This research was funded by FCT/MCTES, grant number UID/QUI/50006/2020, J.M.P.F.O. (SFRH/BPD/74868/2010) thanks FCT for funding through program DL 57/2016-Norma transitória and M.C. was funded by FCT, grant number SFRH/BPD/100865/2014.

Institutional Review Board Statement: Not applicable.

Informed Consent Statement: Not applicable.

Data Availability Statement: All data generated or analyzed during this study are included in this published article.

Conflicts of Interest: The authors declare no conflict of interest.

References

1. Asadishad, B.; Chahal, S.; Akbari, A.; Cianciarelli, V.; Azodi, M.; Ghoshal, S.; Tufenkji, N. Amendment of Agricultural Soil with Metal Nanoparticles: Effects on Soil Enzyme Activity and Microbial Community Composition. *Environ. Sci. Technol.* **2018**, *52*, 1908–1918. [CrossRef] [PubMed]
2. Kah, M.; Hofmann, T. Nanopesticide research: Current trends and future priorities. *Environ. Int.* **2014**, *63*, 224–235. [CrossRef] [PubMed]
3. Pradhan, S.; Mailapalli, D.R. Nanopesticides for Pest Control. *Sustain. Agric. Rev.* **2020**, *8*, 43–74. [CrossRef]
4. Prasad, R.; Bhattacharyya, A.; Nguyen, Q. Nanotechnology in Sustainable Agriculture: Recent Developments, Challenges, and Perspectives. *Front. Microbiol.* **2017**, *8*, 165–181. [CrossRef] [PubMed]
5. Mariz-Ponte, N.; Sario, S.; Mendes, R.J.; Correia, C.V.; Moutinho-Pereira, J.; Correia, C.M.; Santos, C. $TiSiO_4$ nanoparticles can stimulate plant growth and the photosynthetic pigments on lettuce crop. *Agriculture/Pol'nohospodárstvo* **2020**, *66*, 148–160. [CrossRef]

6. Giraldo, J.P.; Landry, M.P.; Faltermeier, S.M.; McNicholas, T.P.; Iverson, N.M.; Boghossian, A.A.; Reuel, N.F.; Hilmer, A.J.; Sen, F.; Brew, J.A.; et al. Plant nanobionics approach to augment photosynthesis and biochemical sensing. *Nat. Mater.* **2014**, *13*, 400–408. [CrossRef]
7. Lyu, S.; Wei, X.; Chen, J.; Wang, C.; Wang, X.; Pan, D. Titanium as a Beneficial Element for Crop Production. *Front. Plant Sci.* **2017**, *8*, 597. [CrossRef] [PubMed]
8. Rastogi, A.; Zivcak, M.; Sytar, O.; Kalaji, H.M.; He, X.; Mbarki, S.; Brestic, M. Impact of Metal and Metal Oxide Nanoparticles on Plant: A Critical Review. *Front. Chem.* **2017**, *5*, 78. [CrossRef]
9. Yang, Z.; Chen, J.; Dou, R.; Gao, X.; Mao, C.; Wang, L. Assessment of the Phytotoxicity of Metal Oxide Nanoparticles on Two Crop Plants, Maize (*Zea mays* L.) and Rice (*Oryza sativa* L.). *Int. J. Environ. Res.* **2015**, *12*, 15100–15109. [CrossRef]
10. Mariz-Ponte, N.; Dias, C.M.; Silva, A.M.; Santos, C.; Silva, S. Low levels of TiO_2-nanoparticles interact antagonistically with Al and Pb alleviating their toxicity. *Plant Physiol. Biochem.* **2021**, *167*, 1–10. [CrossRef]
11. Cox, A.; Venkatachalam, P.; Sahi, S.; Sharma, N. Silver and titanium dioxide nanoparticle toxicity in plants: A review of current research. *Plant Physiol. Biochem.* **2016**, *107*, 147–163. [CrossRef]
12. Luttrell, T.; Halpegamage, S.; Tao, J.; Kramer, A.; Sutter, E.; Batzill, M. Why is anatase a better photocatalyst than rutile?—Model studies on epitaxial TiO_2 films. *Sci. Rep.* **2014**, *4*, 1–8. [CrossRef] [PubMed]
13. Oi, L.E.; Choo, M.Y.; Lee, H.V.; Ong, H.C.; Abd Hamid, S.B.; Juan, J.C. Recent advances of titanium dioxide (TiO_2) for green organic synthesis. *Rsc Adv.* **2016**, *6*, 108741–108754. [CrossRef]
14. Silva, S.; Oliveira, H.; Craveiro, S.C.; Calado, A.J.; Santos, C. Pure anatase and rutile + anatase nanoparticles differently affect wheat seedlings. *Chemosphere* **2016**, *151*, 68–75. [CrossRef]
15. Silva, S.; Pinto, G.; Santos, C. Low doses of Pb affected *Lactuca sativa* photosynthetic performance. *Photosynthetica* **2017**, *55*, 50–57. [CrossRef]
16. Larue, C.; Khodja, H.; Herlin-Boime, N.; Brisset, F.; Flank, A.M.; Fayard, B.; Chaillou, S.; Carrière, M. Investigation of titanium dioxide nanoparticles toxicity and uptake by plants. *J. Phys. Conf. Ser.* **2011**, *304*, 012057. [CrossRef]
17. Arshad, M.; Nisar, S.; Gul, I.; Nawaz, U.; Irum, S.; Ahmad, S.; Sadat, H.; Mian, I.A.; Ali, S.; Rizwan, M.; et al. Multi-element uptake and growth responses of Rice (*Oryza sativa* L.) to TiO_2 nanoparticles applied in different textured soils. *Ecotox. Environ. Safe.* **2021**, *215*, 112149. [CrossRef] [PubMed]
18. Jacob, D.L.; Borchardt, J.D.; Navaratnam, L.; Otte, M.L.; Bezbaruah, A.N. Uptake and translocation of Ti from nanoparticles in crops and wetland plants. *Int. J Phytoremediat.* **2013**, *15*, 142–153. [CrossRef]
19. Deng, Y.; Petersen, E.J.; Challis, K.E.; Rabb, S.A.; Holbrook, R.D.; Ranville, J.F.; Nelson, B.C.; Xing, B. Multiple method analysis of TiO_2 nanoparticle uptake in rice (*Oryza sativa* L.) plants. *Environ. Sci. Technol.* **2017**, *51*, 10615–10623. [CrossRef]
20. Amini, S.; Maali-Amiri, R.; Mohammadi, R.; Kazemi-Shahandashti, S.S. cDNA-AFLP analysis of transcripts induced in chickpea plants by TiO_2 nanoparticles during cold stress. *Plant Physiol. Biochem.* **2017**, *111*, 39–49. [CrossRef]
21. Landa, P.; Vankova, R.; Andrlova, J.; Hodek, J.; Marsik, P.; Storchova, H.; White, J.C.; Vanek, T. Nanoparticle-specific changes in *Arabidopsis thaliana* gene expression after exposure to ZnO, TiO_2, and fullerene soot. *J. Hazard Mater.* **2012**, *241*, 55–62. [CrossRef] [PubMed]
22. Palmqvist, N.G.; Bejai, S.; Meijer, J.; Seisenbaeva, G.A.; Kessler, V.G. Nano titania aided clustering and adhesion of beneficial bacteria to plant roots to enhance crop growth and stress management. *Sci. Rep.* **2015**, *5*, 10146. [CrossRef] [PubMed]
23. Missaoui, T.; Smiri, M.; Chmingui, H.; Hafiane, A. Effects of nanosized titanium dioxide on the photosynthetic metabolism of fenugreek (*Trigonella foenum-graecum* L.). *Comptes Rendus Biol.* **2017**, *340*, 499–511. [CrossRef] [PubMed]
24. Maroufpoor, N.; Mousavi, M.; Hatami, M.; Rasoulnia, A.; Lajayer, B.A. Mechanisms involved in stimulatory and toxicity effects of nanomaterials on seed germination and early seedling growth. In *Advances in Phytonanotechnology; From Synthesis to Application*; Academic Press: Cambridge, MS, USA, 2019; pp. 153–181.
25. Abbasi Khalaki, M.; Moameri, M.; Asgari Lajayer, B.; Astatkie, T. Influence of nano-priming on seed germination and plant growth of forage and medicinal plants. *Plant Growth Regul.* **2021**, *93*, 13–28. [CrossRef]
26. Lei, Z.; Mingyu, S.; Xiao, W.; Chao, L.; Chunxiang, Q.; Liang, C.; Hao, H.; Xiaoqing, L.; Fashui, H. Antioxidant stress is promoted by nano-anatase in spinach chloroplasts under UV-B radiation. *Biol. Trace Elem. Res.* **2008**, *121*, 69–79. [CrossRef] [PubMed]
27. Li, J.; Naeem, M.S.; Wang, X.; Liu, L.; Chen, C.; Ma, N.; Zhang, C. Nano-TiO_2 is not phytotoxic as revealed by the oilseed rape growth and photosynthetic apparatus ultra-structural response. *PLoS ONE* **2015**, *10*, e0143885. [CrossRef] [PubMed]
28. Gao, F.; Liu, C.; Qu, C.; Zheng, L.; Yang, F.; Su, M.; Hong, F. Was improvement of spinach growth by nano-TiO_2 treatment related to the changes of RuBisCO activase? *Biometals* **2008**, *21*, 211–217. [CrossRef]
29. Tan, W.; Du, W.; Darrouzet-Nardi, A.J.; Hernandez-Viezcas, J.A.; Ye, Y.; Peralta-Videa, J.R.; Gardea-Torresdey, J.L. Effects of the exposure of TiO_2 nanoparticles on basil (*Ocimum basilicum*) for two generations. *Sci. Total Environ.* **2018**, *26*, 240–248. [CrossRef]
30. Wu, B.; Zhu, L.; Le, X.C. Metabolomics analysis of TiO_2 nanoparticles induced toxicological effects on rice (*Oryza sativa* L.). *Environ. Pollut.* **2017**, *230*, 302–310. [CrossRef]
31. Rastogi, A. Industrial Nanoparticles and Their Influence on Gene Expression in Plants. In *Nanomaterials in Plants, Algae and Microorganisms*; Academic Press: London, UK, 2019; pp. 89–101.
32. Kataria, S.; Jain, M.; Rastogi, A.; Živčák, M.; Brestic, M.; Liu, S.; Tripathi, D.K. Role of nanoparticles on photosynthesis: Avenues and applications. In *Nanomaterials in Plants, Algae and Microorganisms*; Academic Press: London, UK, 2019; pp. 103–127.

33. Sharma, S.; Sahu, B.; Srinivasan, S.; Singh, M.; Govindasamy, J.; Shanmugam, V. Effect of galvanotaxic graphene oxide on chloroplast activity: Interaction quantified with Biolayer-Interferometry coupled confocal microscopy. *Carbon* **2020**, *162*, 147–156. [CrossRef]
34. Hu, J.; Wu, X.; Wu, F.; Chen, W.; Zhang, X.; White, J.C.; Li, J.; Wan, Y.; Liu, J.; Wang, X. TiO_2 nanoparticle exposure on lettuce (*Lactuca sativa* L.): Dose-dependent deterioration of nutritional quality. *Environ. Sci. Nano* **2020**, *7*, 501–513. [CrossRef]
35. Giorgetti, L. Effects of nanoparticles in plants: Phytotoxicity and genotoxicity assessment. In *Nanomaterials in Plants, Algae and Microorganisms*; Academic Press: London, UK, 2019; pp. 65–87.
36. Boxall, A.B.; Tiede, K.; Chaudhry, Q. Engineered nanomaterials in soils and water: How do they behave and could they pose a risk to human health? *Nanomedicine* **2007**, *2*, 919–927. [CrossRef] [PubMed]
37. Dias, M.C.; Santos, C.; Pinto, G.; Silva, A.M.; Silva, S. Titanium dioxide nanoparticles impaired both photochemical and non-photochemical phases of photosynthesis in wheat. *Protoplasma* **2019**, *256*, 69–78. [CrossRef]
38. Klughammer, C.; Schreiber, U. Complementary PS II quantum yields calculated from simple fluorescence parameters measured by PAM fluorometry and the Saturation Pulse method. *PAM Appl. Notes* **2008**, *1*, 201–247.
39. Murchie, E.H.; Lawson, T. Chlorophyll fluorescence analysis: A guide to good practice and understanding some new applications. *J. Exp. Bot.* **2013**, *64*, 3983–3998. [CrossRef] [PubMed]
40. Sims, D.A.; Gamon, J.A. Relationships between leaf pigment content and spectral reflectance across a wide range of species, leaf structures and developmental stages. *Remote Sens. Environ.* **2002**, *81*, 337–354. [CrossRef]
41. Irigoyen, J.J.; Einerich, D.W.; Sánchez-Díaz, M. Water stress induced changes in concentrations of proline and total soluble sugars in nodulated alfalfa (*Medicago sativd*) plants. *Physiol. Plant.* **1992**, *84*, 55–60. [CrossRef]
42. Osaki, M.; Shinano, T.; Tadano, T. Redistribution of carbon and nitrogen compounds from the shoot to the harvesting organs during maturation in field crops. *Soil Sci. Plant Nutr.* **1991**, *37*, 117–128. [CrossRef]
43. Borowski, J.M.; Galli, V.; da Silva Messias, R.; Perin, E.C.; Buss, J.H.; e Silva, S.D.D.A.; Rombaldi, C.V. Selection of candidate reference genes for real-time PCR studies in lettuce under abiotic stresses. *Planta* **2014**, *239*, 1187–1200. [CrossRef]
44. Livak, K.J.; Schmittgen, T.D. Analysis of relative gene expression data using real-time quantitative PCR and the $2-\Delta\Delta CT$ method. *Methods* **2001**, *25*, 402–408. [CrossRef]
45. Wang, X.P.; Yang, X.Y.; Chen, S.Y.; Li, Q.Q.; Wang, W.; Hou, C.J.; Gao, X.; Wang, L.; Wang, S.C. Zinc Oxide Nanoparticles Affect Biomass Accumulation and Photosynthesis in *Arabidopsis*. *Front. Plant Sci.* **2016**, *6*, 1243. [CrossRef] [PubMed]
46. Servin, A.D.; Morales, M.I.; Castillo-Michel, H.; Hernandez-Viezcas, J.A.; Munoz, B.; Zhao, L.; Nunez, J.E.; Peralta-Videa, J.R.; Gardea-Torresdey, J.L. Synchrotron verification of TiO_2 accumulation in cucumber fruit: A possible pathway of TiO_2 nanoparticle transfer from soil into the food chain. *Environ. Sci. Technol.* **2013**, *47*, 11592–11598. [CrossRef] [PubMed]
47. Song, U.; Jun, H.; Waldman, B.; Roh, J.; Kim, Y.; Yi, J.; Lee, E.J. Functional analyses of nanoparticle toxicity: A comparative study of the effects of TiO_2 and Ag on tomatoes (*Lycopersicon esculentum*). *Ecotoxicol. Environ. Saf.* **2013**, *93*, 60–67. [CrossRef] [PubMed]
48. Song, U.; Shin, M.; Lee, G.; Roh, J.; Kim, Y.; Lee, E. Functional Analysis of TiO_2 Nanoparticle Toxicity in Three Plant Species. *Biol. Trace Elem. Res.* **2013**, *155*, 93–103. [CrossRef] [PubMed]
49. Raliya, R.; Nair, R.; Chavalmane, S.; Wang, W.N.; Biswas, P. Mechanistic evaluation of translocation and physiological impact of titanium dioxide and zinc oxide nanoparticles on the tomato (*Solanum lycopersicum* L.) plant. *Metallomics* **2015**, *7*, 1584–1594. [CrossRef] [PubMed]
50. Zhori, A.; Meco, M.; Brandl, H.; Bachofen, R. In situ chlorophyll fluorescence kinetics as a tool to quantify effects on photosynthesis in *Euphorbia cyparissias* by a parasitic infection of the rust fungus *Uromyces pisi*. *BMC Res. Notes* **2015**, *8*, 698. [CrossRef]
51. Gao, F.; Hong, F.; Liu, C.; Zheng, L.; Su, M.; Wu, X.; Yang, F.; Wu, C.; Yang, P. Mechanism of nano-anatase TiO_2 on promoting photosynthetic carbon reaction of spinach. *Biol. Trace Elem. Res.* **2006**, *111*, 239–253. [CrossRef]
52. Schreiber, U.; Bilger, W.; Neubauer, C. Chlorophyll fluorescence as a nonintrusive indicator for rapid assessment of in vivo photosynthesis. In *Ecophysiology of Photosynthesis*; Springer: Berlin/Heidelberg, Germany, 1995; pp. 40–70. [CrossRef]
53. Killi, D.; Haworth, M. Diffusive and metabolic constraints to photosynthesis in quinoa during drought and salt stress. *Plants* **2017**, *6*, 49. [CrossRef]
54. Bradfield, S.J. Influence of TiO_2 Engineered Nanoparticles on Photosynthetic Efficiency and Contaminant Uptake. Master's Thesis, Southern Illinois University at Carbondale, Carbondale, IL, USA, 2015.
55. Conway, J.R.; Beaulieu, A.L.; Beaulieu, N.L.; Mazer, S.J.; Keller, A.A. Environmental stresses increase photosynthetic disruption by metal oxide nanomaterials in a soil-grown plant. *ACS Nano* **2015**, *9*, 11737–11749. [CrossRef]
56. Linglan, M.; Chao, L.; Chunxiang, Q.; Sitao, Y.; Jie, L.; Fengqing, G.; Fashui, H. RuBisCO activase mRNA expression in spinach: Modulation by nanoanatase treatment. *Biol. Trace Elem. Res.* **2008**, *122*, 168–178. [CrossRef]
57. Couée, I.; Sulmon, C.; Gouesbet, G.; El Amrani, A. Involvement of soluble sugars in reactive oxygen species balance and responses to oxidative stress in plants. *J. Exp. Bot.* **2006**, *57*, 449–459. [CrossRef] [PubMed]
58. Asli, S.; Neumann, P.M. Colloidal suspensions of clay or titanium dioxide nanoparticles can inhibit leaf growth and transpiration via physical effects on root water transport. *Plant Cell Environ.* **2009**, *32*, 577–584. [CrossRef] [PubMed]
59. Tumburu, L.; Andersen, C.; Rygiewicz, P.; Reichman, J. Phenotypic and genomic responses to titanium dioxide and cerium oxide nanoparticles in *Arabidopsis* germinants. *Environ. Toxicol. Chem.* **2015**, *34*, 70–83. [CrossRef] [PubMed]
60. Xue, G.P.; McIntyre, C.L.; Glassop, D.; Shorter, R. Use of expression analysis to dissect alterations in carbohydrate metabolism in wheat leaves during drought stress. *Plant Mol. Biol.* **2008**, *67*, 197–214. [CrossRef] [PubMed]